THE MOVING WEB INSTABILITY CAUSED BY THE BENDING DEFLECTION OF THE SUPPORT IDLE ROLLER

By

Li'e Ma, Mingyue Shao, Jimei Wu, Shanhui Liu, and Dingqiang Liu
The Institute of Printing and Packaging Engineering
Xi'an University of Technology
CHINA

ABSTRACT

The moving web is transported through a lot of rollers in the roll to roll process machines. These rollers are usually driven rollers, dancer rollers and idle rollers. The number of the idle roller is the largest in the roll to roll process machines. The kind of roller is a thin and long part. The bending deflection can be produced by the own gravity and the web tension. The influences on the deflection of the idle rollers by the web tension, gravity, shoulder length and wall thickness are analyzed. The investigation is focused on the dynamics of the idle roller and the web stability. The relationships between the roller dynamic and the speed and tension of the web are developed. The effect on the instability by the diameter of the idle roller, the length of the idle roller, the roller wall thickness, the surface properties of the roller and the web are discussed. The best parameter combinations of the web and roller are given. The results show that the guide rollers dynamic characteristics have a direct impact on the web motion stability.

NOMENCLATURE

A	Nominal cross-sectional area of web
B	Viscous friction coefficient
C, D	Integration constant
d_i	Diameters of rollers
E	Elastic modulus of web material
$f_{i\text{-}1}$	Friction between web and idle roller
I	Moment of inertia
L	Width of web
l	Length of roller
$N_{i\text{-}1}$	Normal force on roller
T	Web tension
$T_{i\text{-}1}$	Web tension at the idle roller (i-1) input side
T_i	Web tension at the idle roller (i-1) output side

Δv Speed difference between web and idle roller
$v_{i\text{-}1}$ Web speed
$v_{r,i}$ Peripheral speed of idle roller
w'' Angular velocity
w' Angular displacement
w Deflection of web
μ Friction coefficient
μ' Coulomb friction coefficient
μ_0 Static friction coefficient
θ Wrap angle of idle roller and the web
ρ Density of the material

INTRODUCTION

In gravure printing machine, the guide rollers are important parts to ensure the web stable transfer. During the web transport process, the guide rollers are idle rollers driven by the friction between the web and the rollers. The guide rollers support and guide the transferring web. Mechanical properties of the guide roller have an important influence on the web transfer stability. The surface structure and mechanical properties of the guide rollers can cause web wrinkles, lateral drift and fracture phenomena and can directly affect the processing speed and accuracy of the web in printing process.

Since rotating machinery is used to transport flexible materials (commonly known as webs) over rollers, it is common to observe periodic oscillations in measured signals such as web tension and web transport velocity. These periodic oscillations are more prevalent in the presence of nonideal elements such as eccentric rollers and out-of-round material rolls. Nonideal effects such as backlash and compliance in transmission systems were considered in Ref. [1]. Governing equations for web tension and transport velocity that can accurately predict measured behavior in the presence of nonideal rollers are beneficial in understanding web transport behavior under various dynamic conditions and the design of suitable web tension and speed control systems [2].

Guide roller manufacturing and installation precision have important influence on machining quality of the web. A model of tilted guide rollers with friction was developed by Brake [3]. It was shown that tilted guides produce a change in the web's displacement, slope, bending moment and shear force. One challenge in designing web conveyance systems was controlling the displacement and vibration of the webs by guides without introducing instabilities or higher frequency disturbances from flange impacts. And When the web was conceptually unwrapped from its path, the normal force between the web and a tilted guide had a component that acts in the direction of the web's lateral displacement, resulting in an equivalent force and bending moment acting on the web. The model was validated by measurements, and was compared to a previously existing model of guide tilt. Modeling and controller design for the longitudinal behavior of the web as it is transported on rollers was addressed in several papers [4-7]. The buckling instability of the web when it has taken the form of a cylindrical shell as it transits a roller was studied. A nonlinear finite element method with strain dependent constitutive relations was developed and verified by tests to predict this instability [8].

Hashimoto described the new theoretical model of friction coefficient between uncoated paper-web and steel roller. In the modeling, the paper base was approximated by the linear spring and the surface asperities were

treated as rigid body based on the observation of web surface structure. Introducing the contact mechanics, the mixed friction coefficient is formulated theoretically for a wide range of roller surface velocity [9]. The resonant frequencies of a system of idle rollers and web spans was given by Pagilla [10] using a simple linear model that describes the web between two driven rollers. The guide roller deflection and the structural optimization were analyzed by using the finite element analysis software. In this process the influence of the wall thickness of the guide roller on the web deflection were also studied [11-12].

The influence of the shoulder length and web tension on the deflection is not studied. In this paper, the deflection problems, the dynamic properties of the guide roller and how the guide roller deflection affects the guide roller dynamic properties are developed. Flexural deformation of the guide roller with different shoulder lengths, different web tensions and wall thicknesses are analyzed under the web tension and the roller gravity using numerical of deflection. The time domain responses under uneven quality of guide rollers in diameter are obtained. The dynamic flexural deformation law and maximum deflection of the guide roller structure are given. The dynamic properties of the web transfer system at the guide roller are developed. The tension variation when web passing through the roller and the speed differences between the web and guide roller are discussed.

DEFLECTION OF THE IDLE ROLLER

Theoretical analysis on the deflection of the idle rollers

During the web transport process, the guide rollers are driven by the surface friction between the web and the idle rollers. Suppose that the web width is *L*, the web tension is *T*, the wrap angle of the idle roller and the web is θ and the surface pressure of the idle roller produced by the motion web is q_s. The idle roller resultant surface pressure is converted into the line pressure q to study the bending deflection of idle roller [11]. The relationship between them is shown in Figure 1.

$$q_s = \frac{2T\sin\frac{\theta}{2}}{R\theta} \quad \{1\}$$

$$q = 2T\sin\frac{\theta}{2} \quad \{2\}$$

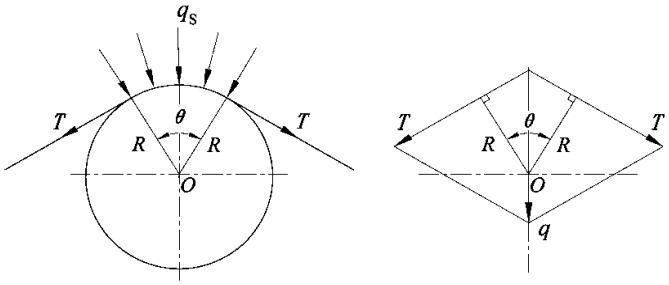

Figure 1 – Web Tension and Guide Roller Pressure

The mechanical model and the composition of the idle rollers are shown in Figure 2. The idle roller consist of the journal 1, the shoulder 2, the plug 3 and the cylinder 4. The diameter, the length and the moment of inertia of them are as d_1, d_2, d_3, and l_1, l_2, l_3 and I_1, I_2, I_3. The elastic modulus and density of the journal 1, shoulder 2 and plug 3 are E_1 and ρ_1. The outer diameter and the inner diameter of the cylinder 4 are d_4 and d_5. The length, the moment of inertia, the elastic modulus and the density of the cylinder 4 are l_4, I_4, E_2 and ρ_2, respectively.

The total mass of the idle roller is simplified as concentration force *G* loaded in the middle of the idle rollers. *DF* segment is suffered uniform line load q which represents web line pressure on the idle roller.

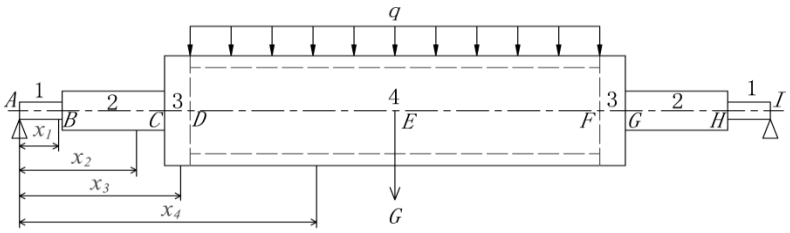

Figure 2 – Mechanical Model of Idle Roller

The structure of the idle roller is symmetrical. According to the static equilibrium conditions we can get the support reactions at both ends.

$$R_{\mathrm{A}} = R_{\mathrm{I}} = \frac{1}{2}R \qquad \{3\}$$

where *R* is the total reaction force at the bearing.

$$R = ql_4 + G$$

The angular displacement and the deflection of *AB*, *BC* and *CD* segment. The angular displacement equations and the deflection equations of *AB*, *BC* and *CD* segment [13] are as follows:

$$\begin{aligned} E_i I_i w_i' &= \frac{1}{4}Rx_i^{\,2} + C_i \\ E_i I_i w_i &= \frac{1}{12}Rx_i^{\,3} + C_i x_i + D_i \end{aligned} \qquad \{4\}$$

where w_i' and w_i is the angular displacement and the deflection of the *i*th segment of the guide roller. C_i and D_i is the integration constant. i =1,2,3.

The angular displacement and the deflection of DE segment under the web tension. The angular displacement equation and the deflection equation of *DE* segment under the web tension are

$$E_2 I_4 w_4' = \frac{1}{4} R x_4^{\,2} - \frac{q\left(x_4 - l_1 - l_2 - l_3\right)^3}{6} + C_4$$

$$E_2 I_4 w_4 = \frac{1}{12} R x_4^{\,3} - \frac{q\left(x_4 - l_1 - l_2 - l_3\right)^4}{24} + C_4 x_4 + D_4 \qquad \{5\}$$

where w_4' and w_4 is the angular displacement and the deflection of *BC* segment. C_4 and D_4 is integration constant.

In this situation the total reaction force at roller bearing is

$$R = qL = ql_4 \qquad \{6\}$$

The structure and the load of the idle roller are symmetrical. So the maximum bending deflection is at the center of the idle roller, that is $x_4 = \frac{1}{2} l_4$. According to the formula {4} ~ {6} the maximum deflection of the idle roller caused by the web tension can be obtained.

$$\left|w_{\max}\right|_1 = \frac{4q\left(l_4/2\right)^4 - q\left(l_4/2 - l_1 - l_2 - l_3\right)^4 + 24C_4 l_4 + 24D_4}{24E_2 I_4} \qquad \{7\}$$

Using the equation {2} into {7}, we obtain

$$\left|w_{\max}\right|_1 = \frac{2T\sin\frac{\theta}{2}\cdot\left[4\left(l_4/2\right)^4 - \left(l_4/2 - l_1 - l_2 - l_3\right)^4\right] + 24C_4 l_4 + 24D_4}{24E_2 I_4} \qquad \{8\}$$

The angular displacement and the deflection of *DE* segment under the force of gravity. The force of roller gravity is simplified as concentrated loading in the middle of the idle rollers. In this situation the *DF* segment is only under idle roller gravity *G* and the total reaction force at roller bearing is

$$R = G \qquad \{9\}$$

The angular displacement equation and the deflection equation of *DE* segment under the force of gravity are

$$E_2 I_4 w_4' = \frac{1}{4} G x_4^{\,2} + C_4$$
$$E_2 I_4 w_4 = \frac{1}{12} G x_4^{\,3} + C_4 x_4 + D_4 \qquad \{10\}$$

We obtain the maximum deflection of idle roller under its own weight by the superposition. The maximum deflection of the idle roller is:

$$\left|w_{\max}\right|_2 = w_1 + w_2 + w_1' l_2 + w_3 + w_2' l_3 + w_4 + w_3' l_4 / 2 \qquad \{11\}$$

The maximum deflection of the idle rollers under the web tension and its weight. The maximum deflection of the idle roller under the web tension and its weight can be obtained by adding method. The maximum deflection is

$$\left|w_{\max}\right| = \left|w_{\max}\right|_1 + \left|w_{\max}\right|_2 \qquad \{12\}$$

Numerical analysis on deflection of the idle roller

The parameters and their value of the idle rollers and web are shown in the Table 1. These parameters are always used in the enterprise.

Wrap Angle (deg)	90
Web Width (mm)	1100
Diameter of Journal 1 (mm)	21
Length of Journal 1 (mm)	33
Diameter of Shoulder 2 (mm)	40
Length of Shoulder 2 (mm)	100,110,120,130,140, 150,160
Diameter of Plug 3 (mm)	120
Length of Plug 3 (mm)	60
Outer Diameter of Cylinder 4 (mm)	120
Inner Diameter of Cylinder 4 (mm)	111,112,113
Length of Cylinder 4 (mm)	1100
Elastic Modulus (GPa)	210
Density ($kg/m^{3)}$	7850
Elastic Modulus(GPa)	70
Density(kg/m^3)	2700

Table 1 – The Idle Rollers and Web Parameters

Influence on the deflection of the idle rollers by the web tension. When the length of the shoulder is 100 mm, 110 mm, 120 mm, 130 mm, 140 mm, 150 mm and 160 mm respectively, according to the formula {9}, {13} and {14}, the deflections of the guide roller with wall thickness 4.5 mm are shown in Figure 3.

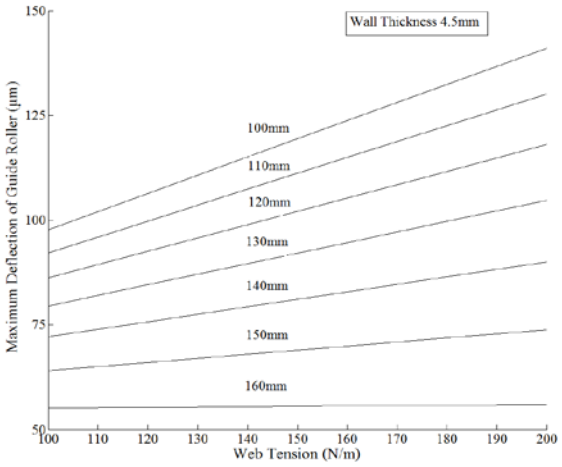

Figure 3 – Deflection Curve Diagram of Web Tension and Guide Rollers

With the increasing of the web tension, the deflection of the guide roller is increasing; the greater of the shoulder length, the smaller of the deflection amplitude increases with the tension. However, increasing the length of the shoulder, the moment inertia of the idle roller is also increasing and the sensitivity of the rotation is reducing. With the increase in web tension the idle roller deflection also increases; when the web tension is constant, the idle roller deflection becomes smaller with the length of the shoulder increasing; when the shaft shoulder length is 160 mm, the idle roller deflection increasing trend with the web tension is slowest.

Influence on the deflection of the idle rollers by the shoulder length and gravity. If the total length is same, the idle roller's weight increases with the increasing of the shoulder length. The web tension is generally 30 ~ 300 N/m [14]. Taking web tension of 200 N/m to calculate, when the wall thickness is 4.5 mm, according to the formula {9}, {13} and {14}, we get the relationship of the deflection changing with the shaft shoulder length as shown in Figure 4.

The deflection caused by the weight of the idle roller increases slowly with the increasing of the shaft shoulder length. While the deflection caused by web tension and the total deflection are decreasing. When the shaft shoulder length is 160 mm and the wall thickness of 4.5 mm, the idle roller deflection is smallest. In this situation the maximum deflection is 54.023 μm.

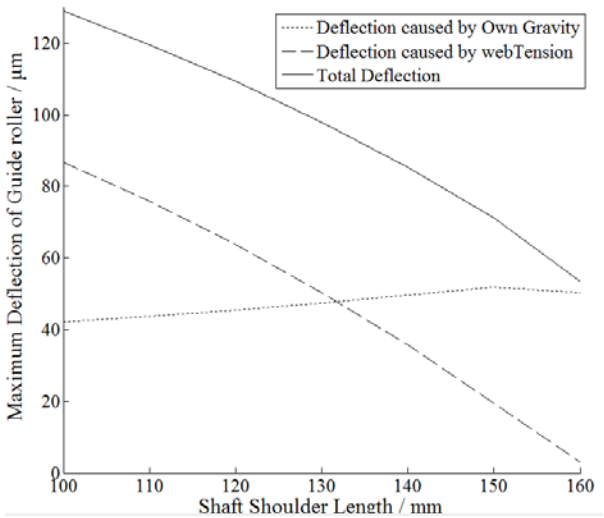

Figure 4 – Maximum Deflection of Guide Roller

Influence on the deflection of the idle rollers by the wall thickness. When the length of the shoulder is 110 mm, the relationships between the web tension and the idle roller deflection with three different wall thicknesses are shown in Figure 5. We can see from the figure that the greater the web tension is, the greater the deflection is. The increasing level is lower with the bigger wall thickness of the guide roller.

The deflections are analyzed in static situation. The results are verified by simulation and test. Next the simulation model will be used to analyze the dynamic situation of the guide roller.

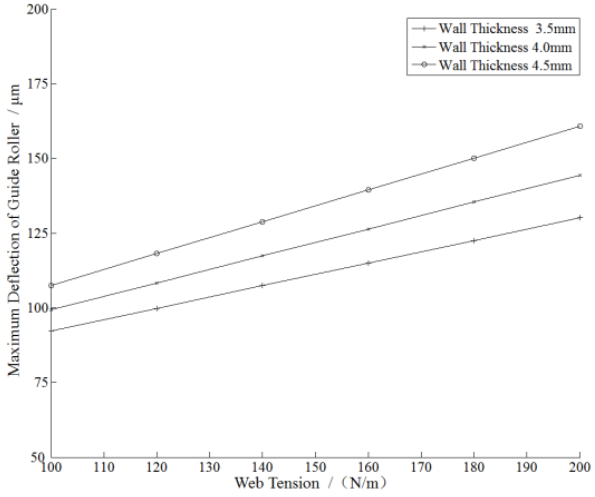

Figure 5 – Maximum Deflection of Guide Roller with Different Wall Thicknesses

DYNAMICS OF THE IDLE ROLLER

In this paper the aim of the dynamic analysis is to get a response when the idle roll is under a time-varying load. When analyzing the guide roller's dynamic characteristics, the roller structure is equivalent to a rotor system. The unbalanced excitation of rotor system is an important area to research rotor dynamics [15].

Unbalanced excitation to the idle roller

The time domain analysis of the guide roller structure is analyzed in unbalanced excitation force which is caused by unbalanced mass *m* in the outer diameter of the roller. This excitation is an eccentric action. The guide roller structure under different rotation speeds will cause different excitation forces.

After the dynamic balancing test, the maximum imbalance mass *m* can be 0.005 kg in the outer diameter of the idle roller. This maximum value is used to analyze the unbalance response analysis. The outer diameter of the idle roller *R* is 0.06 m. so unbalanced mass produce eccentricity e to the idle roller axis.

Unbalanced mass *m* generates a centrifugal force *F* during the rotation of the idle roller shown in Figure 6.

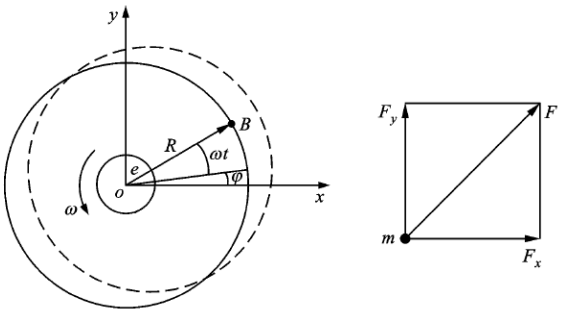

Figure 6 – Excitation Force from Guide Roller Outer Diameter

$$F = mR\omega^2 \quad \{13\}$$

$$F_X = F\cos(\omega t + \phi) \quad \{14\}$$

$$F_Y = F\sin(\omega t + \phi) \quad \{15\}$$

Set the initial state φ is zero. Harmonic response is used to finish the analysis. The relationship between frequency (Hz) and rotation speed (rad/s)

$$f = \omega / 2\pi \quad \{16\}$$

According to the equations {13} and {16} centrifugal force *F* generated by the unbalanced mass can be obtained at different rotation speeds as an incentive force shown in Table 2. The web transfer speed and the corresponding incentive force are as following respectively.

v_1=150 m/min, F_1=10.509 sin41.678t; v_2=200 m/min, F_2 =18.795 sin55.5062t;

v_3=250 m/min, F_3 =29.204 sin69.4292t; v_4=300 m/min, F_4 =42.138 sin83.3569t;

v_5=400 m/min, F_5 =74.879 sin111.107t.

Domain analysis for the idle roller structure

When the printing speed is stable, due to the excitation force caused by the unbalanced quality the idle roller will produce stimulus response. Full method for ANSYS is used to study transient dynamics of the guide roller [16].

The web transmission speed is 400 m/min, the idle roller excitation force is loaded on the node at the middle position of the idle roller, the node at the 1/4 roller and at the both ends of the roller with 4.5 mm wall thickness. The guide roller transient response curves at the three positions are shown in Figure 7.

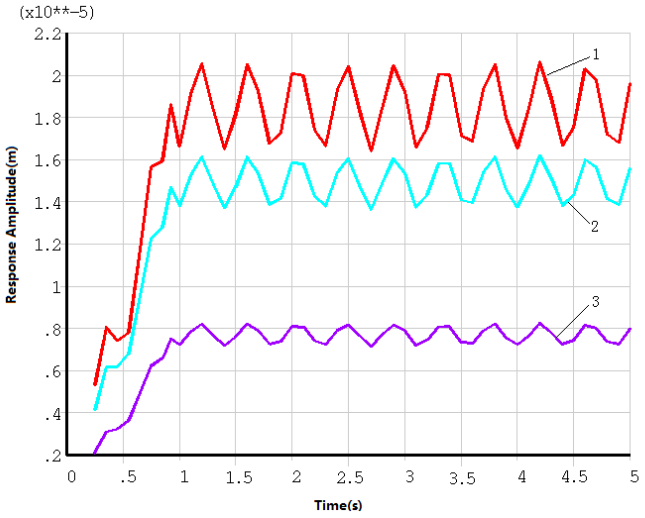

Figure 7 – The Idle Roller Transient Response Curves

In Figure 7 curve 1 is the node response amplitude at the guide roller mid-section node; curve 2 is the node amplitude response at 1/4 position of the roller; curve 3 is the node response amplitude at the end of the guide roller.

The idle roller reaches a steady rotation after 1 second after the unbalanced excitation is applied. Maximum response values at the middle section of the idle roller, so the fluctuation amplitude is the largest. When response value is 18μm, the fluctuation amplitude of the response value is 2.0 μm. And the node of the cylinder end cross-section of transient response at 7.5 μm to fluctuate 1.8 μm.

DYNAMICS OF MOVING WEB AND IDLE ROLLER

Dynamic model

The mechanical model of the web and roller when the web is slipping over the roller (i-1) is shown in Figure 8(a) [17]. v_{i-1} is the web speed , T_{i-1} is web tension to enter the roller (i-1), T_i is web tension in idle roller (i-1) output side, f_{i-1} is the friction between the web and the idle roller and N_{i-1} is the normal force. The friction and normal force can be

computed by considering a micro element in the contact area as shown in Figure 8(b), we obtain the friction force and web tension equation as follow.

$$f_{i-1} = T_i - T_{i-1} = T_{i-1}(e^{\mu\theta_{i-1}} - 1) \qquad \{17\}$$

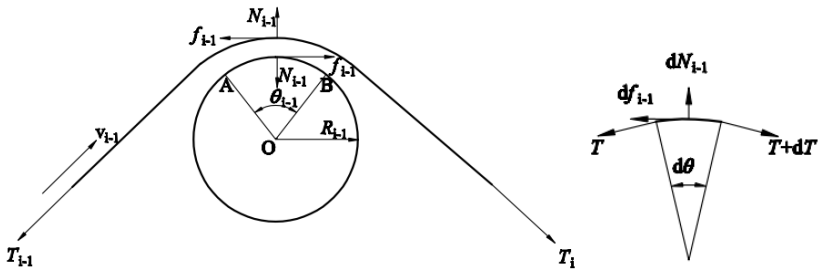

(a) (b)

Figure 8 – The Mechanical Model of Web and Idle Roller

Pure rolling between web and the idle roller

If there is pure rolling between the web and the idle roller, the friction coefficient μ is replaced by coefficient of static friction μ_0. we obtain

$$f_{i-1} = T_{i-1}(e^{\mu_0\theta_{i-1}} - 1) \qquad \{18\}$$

Equation {18} shows the friction force that generates in the contact region between the web and the idle roller. The frictional force f_{i-1} is the traction force by web at the roller i-1.

According to equation {17} we can obtain

$$T_i = T_{i-1}\left(e^{\mu_0\,\theta_{i-1}} - 1\right) \qquad \{19\}$$

Relative sliding between the web and the idle rolls

When the web transport speed v_i and the peripheral speed of the idle roller $v_{r,i}$ ($v_{r,i} = R_i\omega_i$) is not the same, relative sliding is produced between the web and the idle roller. The friction of the web and the idle roller is complex. The friction force is related to the static friction, Coulomb friction and viscous friction and can be expressed as

$$f_i = a \cdot sign\left(v_i - v_{r,i}\right) + b\left(v_i - v_{r,i}\right) + c \cdot \delta\left(v_i - v_{r,i}\right) \qquad \{20\}$$

where a is Coulomb friction force, b is the slope of friction characteristics, c is static friction force.

If the web drives the idle roller $i-1$ to rotate, there is relative sliding. Generally $v_{i-1} > v_{r,i-1}$, according to the formula {20}, we get

$$f_{i-1} = \mu' N_{i-1} + b(v_{i-1} - v_{r,i-1}) \qquad \{21\}$$

The speed difference between the web and the idle roller (the difference between the idle roller circumferential speed and the web transport speed) is as follow.

$$\Delta v = v_{i-1} - v_{r,i-1} = \frac{T_{i-1}}{b}\left(e^{\mu\theta_{i-1}} - 1\right)\left(1 - \frac{\mu'}{\mu}\right) \quad \{22\}$$

Tension Disturbance Caused by the Unbalanced Incentives

Gravure printing machine parameters are used to study and analyze the web and the idle roller dynamic model. The basic parameters of the web and the idle roller are shown in Table 2.

Sectional Area of the Web($m^{2)}$	5.0×10^{-6}
Web Elastic Modulus (Pa)	2.1×10^{9}
Viscous Friction Coefficient (Ns/m)	1,800
Static Friction Coefficient	0.1
Friction Coefficient	0.1
Coulomb friction Coefficient	0.02
Web Tension (N)	200

Table 2 – The Idle Rollers and Web Parameters

The time domain analysis of idle roller structure showed that the idle roller deflection transient response caused by the imbalance incentive can make the web tension disturbance occur. Therefore the idle rollers tension change is based on the law of transient response. Ignoring the tension change under the idle rollers unstable state, according to the curve 1 in Figure 7, considering the imbalance excitation of the idle roller, the web tension equation is

$$T = 200 + 0.42 \times \left[0.2 \times \sin\left(4\pi t - \frac{\pi}{2}\right) + 1.8\right] \quad \{23\}$$

The variation of the web tension is shown in Figure 9.

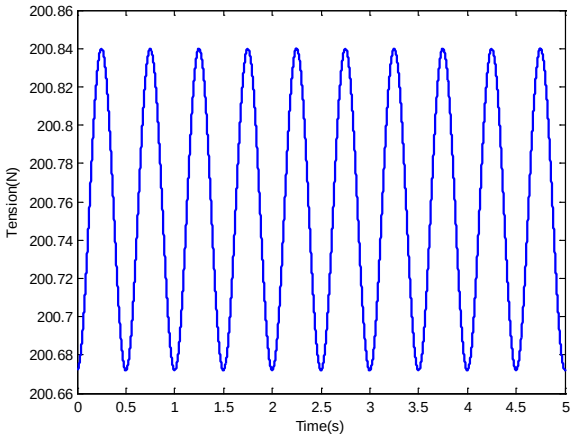

Figure 9 – Tension Disturbance Caused by the Unbalanced Incentives

Influence on Traction Due to Web Tension Disturbance

Considering tension disturbance shown in Figure 9, when the wrap angle is 60 °, according to the parameters in Table 2 of the web and the idle roller, we obtain the traction variation law as in Figure 10.

Figure 10 shows that the traction force affected by the unbalanced incentive also changes with tension disturbance cyclically.

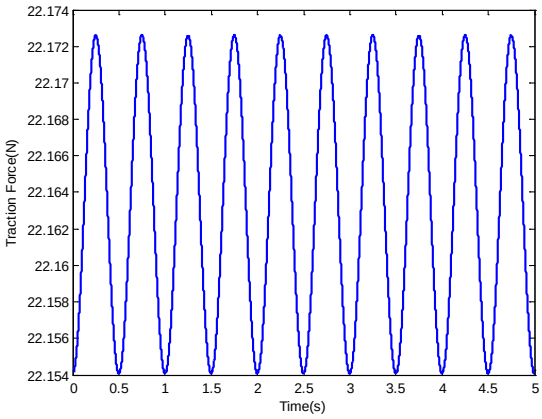

Figure 10 – Traction Force Variation Law

The speed differences analysis between the web and guide roller

The formula{24}shows that the speed difference is related to coefficient of friction , web tension and wrap angle between the web and the idle rollers, but has nothing to the web speed. Letting the wrap angle between the idle roller and web varies from 60 ° to 180 °, according to the formula {24} and parameters in Table 2, we acquire variation law of the wrap angle and the speed difference, as shown in Figure 11.

Figure 11 shows, firstly, the speed difference increases with the wrap angle exponentially, but the magnitude is not large compared to the web transmission speed

(0.83 m / s to 6.67 m / s). Secondly, the speed difference increases with the increase of the friction coefficient. The increase tendency under the friction coefficient $\mu = 0.1$ is the slowest one.

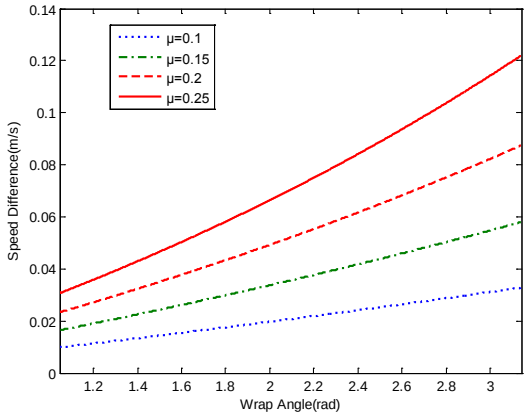

Figure 11 – Speed Difference Due to Friction Coefficient

When the friction coefficient $\mu = 0.1$, the wrap angle θ is 60 °, according to the formula {24} and parameters in Table 2, the variation law of the speed difference and the tension is shown in Figure 12.

Figure 12 shows that the speed difference increases when the tension increases slightly. When μ is 0.15, 0.2 and 0.25 respectively, the conclusions are the same as $\mu = 0.1$. On the whole, the wrap angle and the friction coefficient have obviously impact on speed difference.

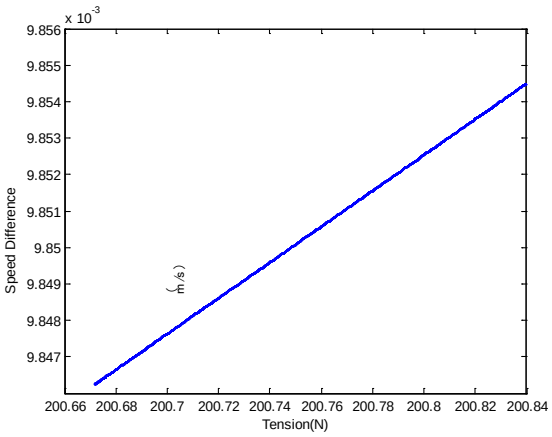

Figure 12 – Speed Difference and the Tension Relations

5 SUMMERY AND CONCLUSIONS

The deflection of the guide roller and the dynamic properties of the moving web and the guide roller are developed. Flexural deformation of the guide roller with different shoulder lengths, different web tensions and three wall thicknesses was analyzed under the web tension and the roller gravity.

The results show that: when the wall thickness of the idle roller is constant, the idle roller deflection increases with the increase in web tension and; when the web tension is constant the idle roller deflection becomes smaller with increasing length of the shoulder; the greater the shoulder length is, the smaller the deflection amplitude is. when the web tension is 200 N/m, with increasing length of the shoulder, the idle roller deflection caused by the gravity shows a slow increase, while the deflection caused by web tension and the total deflection show decrease. The time domain response under uneven quality of guide roller in diameter is obtained.

The dynamic properties of the web transfer system at the guide roller are developed. As a result, the traction force that affected by the idle roller unbalanced incentive also changes with tension disturbance cyclically. On the whole, the wrap angle and the friction coefficient have obviously impacts on speed difference.

The results show that the wall thickness of the guide roller, the roller body length and stub length, web speed and tension are the main factors affecting the mechanical properties of the guide rollers.

ACKNOWLEDGMENTS

This program was supported by the National Natural Science Foundation of China (Grant no. 51305341, 11272253, 11202159) and by the Natural Scientific Research Program of Shaanxi Provincial (Program no. 2014JM2790).

REFERENCES

1. Dwivedula, R. V., “Modeling the Effects of Belt Compliance, Backlash, and Slip on Web Tension and New Methods for Decentralized Control of Web Processing Lines,” Ph.D. Thesis, Oklahoma State University, Stillwater, OK, 2005.
2. Branca, C., Pagilla, P. R., and Reid, K. N., “Governing Equations for Web Tension and Web Velocity in the Presence of Nonideal Rollers,” Journal of Dynamic Systems, Measurement, and Control, Vol.135, No.1, 2013, p. 011018.
3. Brake, M. R., and Wickert, J. A., “Tilted Guides with Friction in Web Conveyance Systems,” International Journal of Solids and Structures, Vol. 47, No. 21, 2010, pp. 2952-2957.
4. Brandenburg, G., “New Mathematical Model for Web Tension and Register Error,” Proceedings of the 3rd International IFAC Conference on Instrumentation and Automation in the Paper, Rubber and Plastics Industries, 1976, pp. 411-438.
5. Whitworth, D., “Tension Variations in Pliable Material in Production Machinery,” Ph.D. Thesis, Department Engineering Production, Loughborough University Technology, 1979, Loughborough, UK.
6. Shelton, J. J., “Dynamic of Web Tension Control with Velocity or Torque,” Proceedings of the American Control Conference, 1986, pp. 1423-1427.
7. Pagilla, P. R., Siraskar, N. B., and Dwivedula, R. V., “Decentralized Control of Web Processing Lines,” IEEE Trans. Control Syst. Technol., Vol.15, No.1, 2007, pp. 106-116.

8. Beisel, J. A., and Good , J. K., “The Instability of Webs in Transport,” Journal of Applied Mechanics, Vol.78, No.1, 2011, pp. 1-7.
9. Hashimoto, H., “Friction Characteristics between Paper and Steel Roller under Mixed Lubrication,” Proceedings of the Institution of Mechanical Engineers Part J – Journal of Engineering Tribology, Vol. 226, No. 12, 2012, pp. 1127-1140.
10. Pagilla, P. R., and Diao, Y., “Resonant Frequencies in Web Process Lines Due to Idle Rollers and Spans,” Journal of Dynamic Systems Measurement and Control, Transactions of the ASME, Vol. 133, No. 6, 2011, p. 061018.
11. Ma, L., Mei, X. S., Wu, J. M., Wan, Q. Q., and Liu, S. H., “The Modeling and Simulation of the Guide Roller in Web Processing System,” 2014 International Conference on Information Science, Electronics and Electrical Engineering, ISEEE 2014, pp.1766-1769.
12. Ma, L., Mei, X. S., Li, Y. F., et, al., “Mechanical Behaviors of Guide Roller in Web Transfer System,” Journal of Xi'an Jiaotong University, Vol. 48, No. 11, 2014, pp. 86-91.
13. Liu, H. W., Mechanics of Materials, Higher Education Press, Beijing, 2005, 176-192.
14. Wu, J. M., Wang, Z. M., and Wang, Y., “Printing Movement Transverse Vibration Properties of Paper Tape,” China Mechanical Engineering, Vol. 20, No. 13, 2009, pp. 1519-1523.
15. Li, C. L., “The Paper Guide Roller Unbalance Calculation and Derivation,” Guangxi Journal of Light Industry, Vol. 1, No. 13, 2007, pp. 53-54.
16. Hu, G. L., Ren J. W., and Long M., ANSYS 13.0 Finite Element Analysis and Practical Tutorial, 2nd ed., National Defense Industry Press, 2012.
17. Dwivedula, R. V., and Pagilla, P. R., “Modeling of Web Slip on a Roller and Its Effect on Web Tension Dynamics,” 2005 ASME International Mechanical Engineering Congress and Explosion, November 1-5, 2005, Orlando, Florida USA.